J Mater Sci: Mater Electron
DOI 10.1007/s10854-011-0382-1

Electrical and optical properties of one-dimensional metallophthalocyanine (M = Fe) thin films grown by thermal evaporation

M. E. Sánchez-Vergara · V. García-Montalvo · J. C. Alonso-Huitrón · A. Rodriguez · O. Jiménez-Sandoval

Received: 10 March 2011 / Accepted: 15 April 2011

Abstract Semiconducting molecular materials based on iron phthalocyanine and diamine ligands have been successfully used to prepare thin films by a thermal evaporation technique. The samples were deposited on corning glass substrates and crystalline silicon wafers and were characterized by FT-IR, UV–Vis, SEM and EDS. The optical parameters have been investigated using spectrophotometric transmission measurements in the 200–1,150 nm wavelength range. The UV–VIS spectra of the films show two well defined absorption bands, namely, the Soret and the Q-band. The values of the optical band gap E_g (direct transitions) calculated from the absorption spectra, ranged between 3.30 and 4.38 eV. The effect of temperature on the conductivity of the films was also evaluated and the electrical transport properties were studied by dc conductivity measurements. The electrical activation energies of the complexes, which were in the range of 0.04–0.64 eV, were calculated from Arrhenius plots.

M. E. Sánchez-Vergara (✉)
Facultad de Ingeniería, Universidad Anáhuac México Norte, Avenida Universidad Anáhuac 46, Col. Lomas Anáhuac, 52786 Huixquilucan, Estado de México
e-mail: elena.sanchez@anahuac.mx

V. García-Montalvo
Instituto de Química, Universidad Nacional Autónoma de México, Circuito Exterior, Ciudad Universitaria, 04510 Mexico, DF, Mexico

J. C. Alonso-Huitrón · A. Rodriguez
Instituto de Investigaciones en Materiales, Universidad Nacional Autónoma de México, A. P. 70-360, Coyoacán, 04510 Mexico, DF, Mexico

O. Jiménez-Sandoval
Centro de Investigación y de Estudios Avanzados del Instituto Politécnico Nacional, Unidad Querétaro, Apartado Postal 1-798, Querétaro, Qro 76001, Mexico

1 Introduction

Metal phthalocyanines (MPc's) have gained considerable attention in recent years due to their successful use in important functional materials in many fields [1], for instance, in gas sensors [2, 3], solar cells [4–6] and non-linear optical devices [7]. They are also widely used as excellent pigments, molecular thermometers and electrochromic displays given their absorption properties in the UV–Vis region. Furthermore, particular derivatives are known to have potential as second-generation photosensitizers for photodynamic therapy (PDT) of cancer due to their strong absorption of the far-red light (600–850 nm) [1, 8]. The assets of MPc's are almost universally based on electron transfer reactions involving their 18 π-electron conjugated ring system. These aromatic macrocyles crystallize as a range of at least fifteen distinct polymorphs [9]. Very often, thin films of phthalocyanines are made by a vacuum evaporation technique which produces highly pure films without decomposition [10]. Typically, thin films exist as either α- or β-phases, which have also been observed in relatively thick (>100 nm in diameter) wires; their electrical conductivities are as low as 10^{-11} –10^{-13} Scm^{-1}. On the other hand, the axial bridge MPc's form a large kind of extensively studied one-dimensional conductors, $[PcML]_n$ (M = Fe, Co, Mn, Ru, Os; L = cyano, pyrazine, tetrazine, bipyridine, etc.) [11, 12]. For this purpose, semi-conducting thin films based on FePc and axial diamine ligands were prepared and their optical and electrical properties studied. The ligands used were ethylenediamine (EDA), 1,4-diaminobutane (BDA) and

Published online: 27 April 2011

2,6-diamineanthraquinone (AqDA). The films were prepared by thermal evaporation and characterized by ellipsometry measurements. The refractive indices and absorption coefficients, parameters of particular interest for the design and fabrication of optoelectronic devices, have been determined for the films as well. The optical band gap was calculated from the Tauc model [13] and the electronic band gap was also estimated.

2 Experimental details

The raw materials for this work were obtained from commercial sources with no purification prior to their use. The (μ-cyano)(phthalocyaninate)iron(III) complex, $[PcFeCN]_n$, was obtained according to the literature [14].

2.1 General procedure

$[PcFeCN]_n$ dissolved in absolute methanol was added to a methanolic solution of the appropriate diamine [ethylenediamine (EDA), 1,4-diaminebutane (BDA) or 2,6-diamineanthraquinone (AqDA)]. The resultant mixture was maintained under reflux and with stirring for about 3 days until a precipitate was obtained. The product was then filtered, washed with distilled water and absolute methanol, to eliminate the unreacted diamine and $[PcFeCN]_n$, respectively, and then dried in vacuum.

2.1.1 PcFe(EDA)CN (Fe1)

0.20 g (0.34 mmol) of $[PcFeCN]_n$ in 15 mL methanol, 15 mL of ethylenedyamine (excess) in 8 mL methanol. Green powder, yield 73%, m.p. 330 °C (dec). MS(FAB^+, DMSO/EtOH) *m/z*: 568 $[C_{34}H_{16}N_8Fe]^+$, 1,255 $[C_{68}H_{47}Fe_2N_{20}]^+$, 1,281 $[C_{69}H_{47}Fe_2N_{21}]^+$.

2.1.2 PcFe(BDA)CN (Fe2)

0.12 g (0.21 mmol) of $[PcFeCN]_n$ in 10 mL methanol, 0.24 g (2.7 mmol) of 1,4-diaminebutane in 10 mL methanol. Green powder, yield 81%, m.p. 345 °C (dec). MS(FAB^+, DMSO/EtOH) *m/z*: 568 $[C_{32}H_{16}N_8Fe]^+$, 655 $[C_{36}H_{27}FeN_{10}]^+$, 680 $[C_{37}H_{27}FeN_{11}]^+$.

2.1.3 PcFe(AqDA)CN (Fe3)

0.20 g (0.34 mmol) of $[PcFeCN]_n$ in 10 mL of methanol, 0.40 g (1.68 mmol) of 2,6-diamineanthraquinone in 10 mL methanol. Green powder, yield 69%, m.p. 335 °C (dec). MS(FAB^+, DMSO/EtOH) *m/z*: 568 $[C_{32}H_{16}N_8Fe]^+$, 805 $[C_{46}H_{24}Fe\ N_{10}O_2]^+$, 831 $[C_{47}H_{24}Fe\ N_{11}O_2]^+$.

2.2 Powder characterization

FT-IR (Nujol mulls and KBr pellets), *Bruker* spectrophotometer, model *Tensor 27*. Mass spectra (FAB+) were measured on a 3-nitrobenzyl alcohol support in the positive ion mode on a Jeol JMS-SX102A instrument.

2.3 Thin-film deposition

A vacuum chamber was used with a diffusion pump and a special molybdenum crucible with a double-grid cover. A quartz fiber was put inside the crucible to avoid the ejection of grains towards the substrate at a temperature of 563 K. The material was deposited on Corning 7059 glass substrates, which were ultrasonically degreased in warm methanol and dried in nitrogen, and on single-crystalline c-Si wafers, which were chemical etched with a *p* solution (10 mL HF, 15 mL HNO_3 and 300 mL H_2O) in order to remove the native oxide from the c-Si surface. The base pressure used in the evaporation process was 10^{-5} torr at room temperature. The crucible-substrate distance was 20 cm.

2.4 Thin-film characterization

Scanning electron microscopy was carried out in a Jeol JSM 5200 CX microscope, using a 5 kV potential for all samples. FT-IR spectroscopy, *Nicolet* spectrophotometer, model *205* (films on silicon substrates). Ultraviolet–visible spectra, *Unicam* spectrophotometer, model *UV300*, in the 190–1,100 nm range, with a 0.5 nm resolution (films on glass substrates). Ellipsometry, *Gaertner Scientific Corporation* ellipsometer, model *L117*, with a He–Ne laser operating at 630 nm (films deposited on silicon wafers). Profilometry, *Dektak* profilometer, model *IIA* (films evaporated on glass substrates). The samples for electrical characterization had a planar distribution. The separation between electrodes was 0.5 mm. The characterization of these samples on glass substrates was performed with a PC-controlled automatic system using a Keithley 230 programmable voltage source, a Keithley 485 pico-ammeter and a LabView-based program.

3 Results and discussion

The (μ-cyano)(phthalocyaninate)iron(III), $[PcMFeCN]_n$, was selected for this study because of its simple synthesis, the possibility of changing the axial ligands and the stability of the iron-macrocyclic ligand bonds. Molecular materials were obtained by replacing one of the cyano groups of the metal ion with the amine species (Fig. 1).

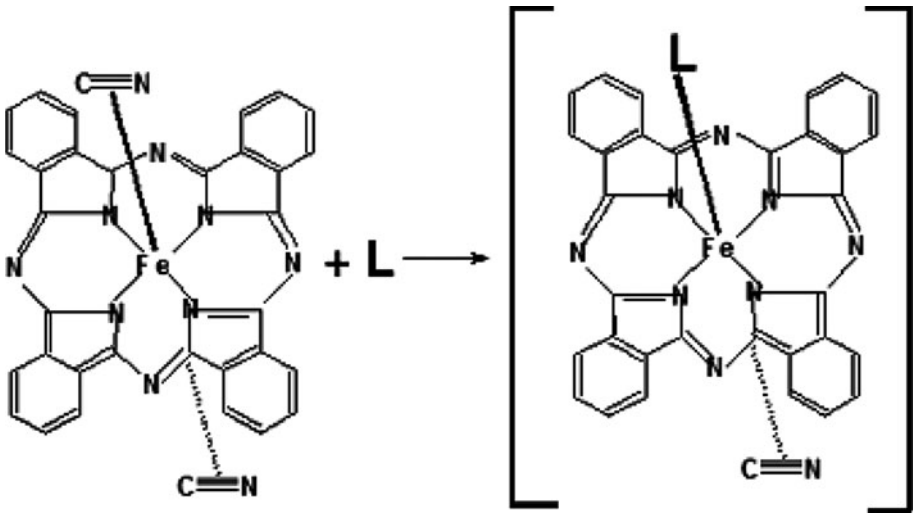

Fig. 1 Chemical structures of the synthesized molecular materials obtained from $[PcFeCN]_n$ L = EDA, BDA, AqDA

Table 1 Characteristic FT-IR bands for powders and thin films of $[PcFeLCN]_n$ (cm^{-1})

Sample	$[PcFeCN]_n$	Fe1		Fe2		Fe3	
	Powder	Powder	Thin film	Powder	Thin film	Powder	Thin film
***ν*(C≡N)**	2,175	2,039	2,031	2,032	2,036	2,044	2,040
***ν*(N–H)**	–	3,217	3,215	3,236	3,234	3,418, 3,327, 3,202	3,421, 3,332, 3,211
***ν*(C=O)**	–	–	–	–	–	1,628	1,622
***ν*(C–H)**	–	2,940	2,942	2,945	2,943	–	–

The FT-IR spectra of powder samples showed the characteristic absorption bands at 1,560, 1,320, 1,140, 1,080, 980, 880 and 740 cm^{-1} of metalphthalocyanine, and also distinguishing stretching bands around 3,400 and 3,330 cm^{-1} indicating the presence of $–NH_2$ groups. An additional small peak appears at 3,211 cm^{-1}, which is attributed to the change of vibrational energy of the amine group when it binds to FePc as it was observed in metalphthalocyanine sensors for amines [15, 16]. The band around 1,720 cm^{-1} corresponds to N–H bending vibrations and the one at 2,940 cm^{-1} to C–H stretching vibrations for the aliphatic chain of the amine ligands (EDA and BDA). Additionally, the sample containing AqDA (**Fe3**) exhibits a strong C=O stretching vibration band at 1,628 cm^{-1}. These features suggest the coordination of the amine ligands to the iron macrocycle, FePc. Table 1 shows characteristic bands for the samples as powders and the corresponding thin films. All the materials display the cyano stretching vibration bands around 2,038 cm^{-1}, indicating only the partial substitution of the C≡N groups. This result contrasts that of the $[PcFe(EDA)]_n$ polymer previously reported [17]. The comparison of the cyano stretching frequency in $[PcFeCN]_n$ indicates a terminal CN group *trans* to the amine binder, as in the reported PcCoLCN monomeric compounds (L = pyridine, 2-methylpyrazine, piperidine, n-butylamine), where the signals for the terminal CN groups are shifted to higher energies in relation to that of $[PcCoCN]_n$ [14]. On the other hand, the comparison between the IR spectra of the synthesized powders and those of the deposited films indicate that there were no significant chemical changes in these materials during the thermal evaporation process to obtain the films. Thus, the deposited films are formed by the same macro-ions as those of the original synthesized powders.

Despite the low solubility of the samples, the FAB^+-mass spectra show fragments with the appropriate isotopic ratio representing the PcFe moiety, $[C_{32}H_{16}N_8Fe]^+$ (568 m/z), and fragments containing the macrocycle and one amine ligand (PcFe/amine), confirming the addition of the amine to the PcFe units. Additionally, in the case of **Fe1**, fragments containing two PcFe and two amines and/or a C≡N group (amine/PcFe/amine/$PcFe^+$, 1,255 m/z and amine/PcFe/amine/PcFe/CN^+ 1,281 m/z) were also found, while in the spectra of **Fe2** and **Fe3**, fragments containing PcFe and the CN group were also observed. All the spectra display additional low intensity signals for heavier fragments up to 1,400 m/z.

An EDS analysis was performed to determine the chemical composition of the novel molecular materials. Figure 2 shows the EDS analysis for PcFe(AqDA)CN (**Fe3**), where the presence of the reference elements for both, donor and acceptor species, is observed. Analogous

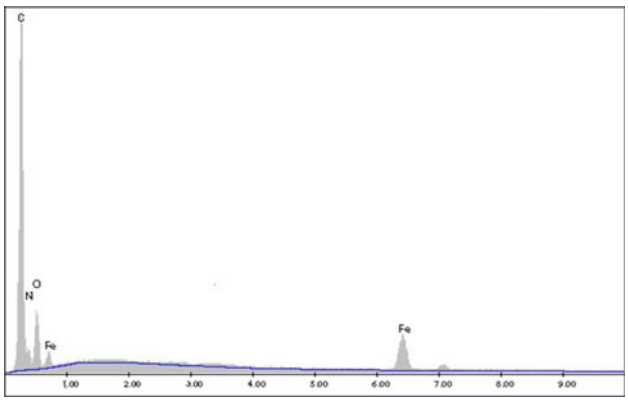

Fig. 2 EDS for PcFe(AqDA)CN (**Fe3**)

results were obtained for the other compounds. The SEM micrographs of the **Fe1** to **Fe3** thin films are shown in Fig. 3. In all cases, the thin films showed an irregular and granular appearance.

The thickness (τ) of the films was determined by ellipsometry and varies from 211 to 635 nm (Table 2). The refractive index (n), which is used to calculate the reflectance (R) percentage from Eq 1, was obtained from ellipsometry measurements as well. The estimated reflectance is lower than 15%, so the optical properties of the thin films can be analyzed according to the Tauc model [13], which was developed to study the optical properties of amorphous semiconductor materials.

$$R = \frac{100\,(n-1)^2}{(n+1)^2}. \tag{1}$$

The optical transmission spectra of the thin-film compounds deposited on Corning 7059 glass were recorded from 200 to 1,150 nm and are shown in Fig. 4. In accordance with their electronic structure, the materials present intense π-π bands in the visible (Q band) and UV (B or Soret band) spectral regions [7]. The Q band, can be attributed to the allowed highest occupied molecular orbital (HOMO)-lowest unoccupied molecular orbital (LUMO) (π-π^*) transition [7]. **Fe1** and **Fe2** have the strongest absorption peaks, around the 680 nm region; the exact position of these bands depends on the particular structure, metal complexation, and peripheral substituents. Metal incorporation induces a decrease in the extinction coefficient for the Q band. For peripherally substituted MPcs, the degenerate Q band shows some splitting due to the reduction in symmetry [7]. The Q-band is shifted to longer wavelengths due to the coordination of the diamine ligands to PcFe. Since the ligands may increase the interfacial distance between PcFe rings, the direct π-π overlap of the macrocycles does not occur and the Q-band is maintained. Then, the presence of this absorption band may be interpreted as an overlap of π orbitals through the ligand, where the electrons are able to transfer energy throughout the structure [12, 18]. The Soret band appears in the region between 310 and 480 nm for the thin films **Fe1**, **Fe2** and

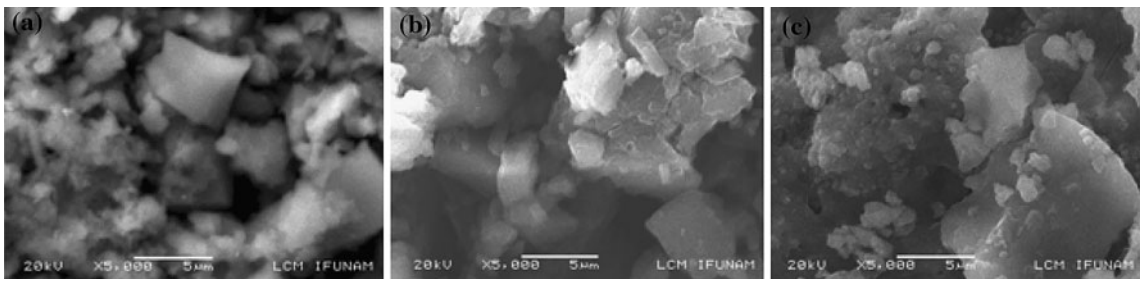

Fig. 3 SEM micrographs of materials **a** Fe1, **b** Fe2 and **c** Fe3, at 5,000×

Table 2 Characteristic parameters of the novel $[PcFeLCN]_n$ thin-films

Sample	σ at 25°C (S cm^{-1})	τ (nm)	Refractive index, n	Reflectance, R (%)	E_{a1}, E_{a2}, E_{a3} (eV)	Eg_i (eV)	Eg_d (eV)
Fe1	3.2×10^{-4}	623	2.435	14.45	0.07 0.04 0.64	1.44	3.30
Fe2	1.8×10^{-5}	635	2.386	13.76	0.12 0.33 0.20	3.42	4.38
Fe3	2.5×10^{-4}	211	1.056	0.074	0.09 0.08 0.53	3.33	4.32

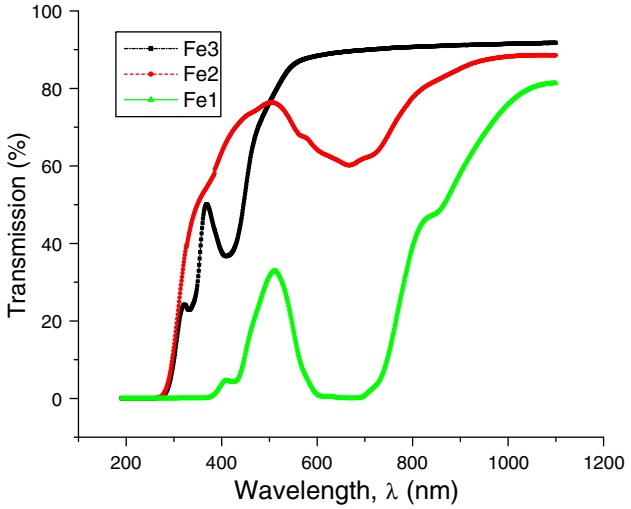

Fig. 4 Transmission spectra of the new $[PcFeLCN]_n$ thin-films

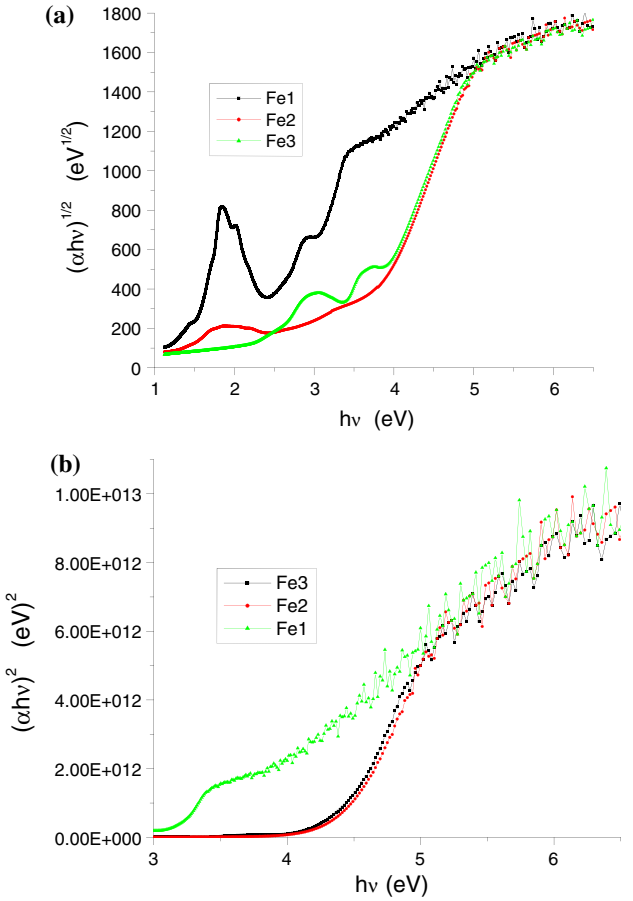

Fig. 5 Absorption plots of the $[PcFeLCN]_n$ thin-films for: **a** indirect and **b** direct transitions

Fe3. The broad absorption band in the UV region is preceded by the ultraviolet absorption band edge of the phthalocyanine moiety [19]. The band around 400 nm is due to electronic transitions between molecules, having an intermediate ionic degree, that conform the synthesized molecular materials. Phthalocyanine thin films absorb light on either side of the blue-green region and may be used as photoconductors. Similar features were observed in works previously undertaken for thin films of phthalocyanine [20, 21] and $PcOCFe(pyz)_2$ and $[PcOCFe(pyz)]_n$ derivatives [12].

The absorption coefficient is defined by the Beer-Lambert law and can be calculated from the optical transmittance [22]. Eq. 2 was used to obtain the absorption coefficient (α) for each wavelength the materials were irradiated with in terms of the transmittance T and thickness τ of the sample.

$$\alpha = -\frac{1}{d}\ln(T) \tag{2}$$

On the other hand, Eq. (3) was used to calculate the photon energy ($h\upsilon$) for each wavelength.

$$E_{\text{photon}} = \frac{h\,c}{\lambda} \tag{3}$$

In order to evaluate the nature of the transition (direct or indirect), the following relation deduced for the domain of fundamental absorption edge [23], was used:

$$\alpha h\upsilon = A(h\upsilon - Eg)^n. \tag{4}$$

In this relation α denotes the absorption coefficient, $h\upsilon$ the photon energy, Eg the band gap energy, n is a number characterizing the transition process and A is a characteristic parameter for respective transitions and can be assumed to be constant within the optical frequency range [10]. For allowed direct transitions $n = ½$, and for allowed indirect transitions $n = 2$. Thus, the optical gaps for both transitions could be determined by the extrapolation to zero of the linear regions of the $(\alpha h\upsilon)^2 = f(h\upsilon)$ and $(\alpha h\upsilon)^{½} = f(h\upsilon)$ plots, Eg_d and Eg_i, respectively (Fig. 5a, b and Table 2) [24]. The straight line nature of the plots over a wide range of photon energies indicates direct and indirect types of transition. To obtain information about direct or indirect interband transitions, the fundamental absorption edge data are analyzed within the framework of the one-electron theory of Bardeen et al. [20]. This theory has been used to analyze the absorption edge data of molecular solids such as phthalocyanine [25]. The absorption ($\alpha \geq 10^4\ \text{cm}^{-1}$) is related to direct band transitions [26].

Figure 5 shows evidence for both direct (E_{gd}) and indirect (E_{gi}) transitions for all thin films. In amorphous semiconductors, the optical transitions are dominated, to a first approximation, by the so-called indirect transitions. In these electronic transitions from states in the valence band to states in the conduction band, there is no conservation of

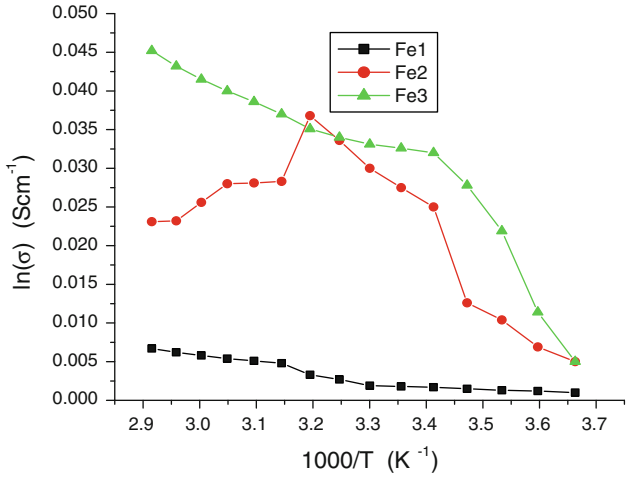

Fig. 6 Electrical conductivity as a function of temperature of Fe1, Fe2 and Fe3

the electronic momentum [27]. However, as can be seen in Fig. 5 and for all the materials, direct transitions are related to a less variable slope in the graph. For the direct transition, the squared absorption coefficient is a linear function of the incident photon energy, which is related to the one-electron theory of Bardeen et al. [20]. The absorption ($\alpha > 10^4$ cm^{-1}) is related to direct interband transitions where the lowest part of the valence band and the highest part in the conduction band share the same wave vector and there is an allowed transition across the band gap. Phonon-electron coupling may help to explain the reduced importance of indirect transitions in these cases. The optical band gap energies, calculated from the Tauc model [13] using the results shown in Fig. 5, are provided in Table 2.

According to thermal decomposition temperatures, electrical conductivities of the materials were measured in the 273–373 K temperature range. By analyzing the shape of $ln\ \sigma = f(1{,}000/T)$ graphs in Fig. 6, useful information regarding the processes occurring in the thin films during the heat treatment can be obtained. The dc conductivity has the general form,

$$\sigma = \sigma_0 \exp\left(-\frac{E_a}{kT}\right). \tag{5}$$

where E_a is the thermal activation energy of the electrical conductivity, σ_0 is the pre-exponential factor depending on the semiconductor nature, and k is Boltzmann's constant. A plot of ln σ versus 1,000/T yields a straight line whose slope can be used to determine the thermal activation energies of the thin films (Fig. 6). Electrical conductivity studies are used to determine thermal activation energy. Calculated values of E_a are shown in Table 2, as well as the electrical conductivity (σ) at 25 °C of the films. Such σ values lie within the semiconductor region (10^{-6}–10^{1} S cm^{-1}) [28]. Our films exhibited lower conductivity values in comparison with FePcCl films deposited onto gold electrodes for which the electrical conductivity was 10^{-3} S cm^{-1} [29]. Nevertheless, the conductivity values obtained for these materials were higher than those for the corresponding pure metallic complexes as reported by Seoudi et al., suggesting that the addition of ligand improves charge transport properties [30]. In inorganic materials the semiconducting properties are mainly caused by thermal excitation, impurities, lattice defects and non-stoichiometry [31]. Holes in the valence band and electrons in the conduction band contribute to the electrical conductivity. Conductivity in phthalocyanines is due to both hopping of holes and charge transport via excited states. In this group of materials it may be observed (Table 2) that **Fe1** is the one that exhibits higher conductivity compared to **Fe2** and **Fe3**.

In general terms, Fig. 6 shows that the curves for all materials are characterized by three portions with different slopes and therefore three activation energies are obtained and given in Table 2; E_{a1} is the intrinsic energy gap and E_{a2} and E_{a3} are the activation energies needed to excite the carriers from the corresponding trap levels to the conduction band. The activation energies of the films are found to decrease with an increase of the substrate temperatures. The thermal activation energy E_{a1} is associated with an intrinsic generation process. This corresponds to the process observed in inorganic semiconductors. It is based on the assumption of electron–hole pair production via thermal transition from a valence band to the conduction band. The assumption of an intrinsic excitation process explains the dependence of the electrical conductivity of phthalocyanine compounds on the constitution of the molecules [31]. The phthalocyanines owe their intrinsic conductivity to the partial charge transfer from the phthalocyanine ring to the central ion and the ligand ethylenediamine, 1,4-diaminebutane and 2,6-diamineanthraquinone. E_{a2} and E_{a3} are the activation energies needed to excite the carriers from the corresponding trap levels to the conduction band and are associated with the impurity conduction [31]. The existence of trap levels in the forbidden energy gap is confirmed by the presence of more than one linear portion in Fig. 6.

4 Conclusions

Thin films of molecular materials of the $[PcFeLCN]_n$ type were deposited by vacuum thermal evaporation. According to their FT-IR spectra, they are formed by the same chemical units as those of the corresponding synthesized powders. Thus, the thermal evaporation process can be, in general, considered as a molecular process. The information obtained from the absorption spectra indicates that

these films absorb light on either side of the blue-green region. The two main absorption bands of metal phthalocyanines are ascribed to the π to π^* transition. Q and B bands correspond to transitions from the highest occupied orbital (for the Q band) and the low occupied orbitals (for the B band) to the lowest excited-state orbitals. The charge transport is expected to be facilitated by this π–π^* overlap. The effect of temperature on conductivity was also evaluated and the thin films show typical semiconducting characteristics. The existence of trap levels is confirmed by the presence of more than one linear portion in the ln σ versus 1,000/T plots. A change in substrate temperature results in a change in the intrinsic activation energy and the electron transport is influenced by the molecular structures of the materials. The value of the calculated activation energies and the order of magnitude of the electrical conductivities suggest that the studied films may be good candidates for their use in electronic devices.

Acknowledgments The authors acknowledge Ing. J. Eleazar Urbina, Fis. Roberto Hernandez and Dr. Margarita Rivera for technical assistance in the EDS and SEM measurements. We wish thank Dr. Jose Ramon Alvarez Bada for the English revision of the manuscript.

References

1. K. Sakamoto, E. Ohno-Okumura, Materials 2 (2009) 1127–1179; doi: 10.3390/ma2031127
2. P. Mashazi, C. Togo, J. Limson, T. Nyokong, J. Porphyrins Phthalocyanines **14**(3), 252–263 (2010)
3. P. Oña-Burgos, M. Casimiro, I. Fernández, A. Valero Navarro, J.F. Fernández Sánchez, A. Segura Carretero, A. Fernández Gutiérrez, Dalton Trans. **39**, 6231–6238 (2010)
4. G. Bottari, G. de la Torre, D. M. Guldi, T. Torres, Chem. Rev. Articles ASAP DOI: 10.1021/cr900254z
5. H. Wang, S. Mauthoor, S. Din, J.A. Gardener, R. Chang, M. Warner, G. Aeppli, D.W. McComb, M.P. Ryan, W. Wu, A.J. Fisher, M. Stoneham, S. Heutz, ACS Nano **4**(7), 3921–3926 (2010)
6. N. Papageorgiou, E. Salomon, T. Angot, J. Layet, L. Giovanelli, G. Le, Lay, Prog. Surf. Sci. **77**, 139–170 (2004)
7. G. de la Torre, P. Vázquez, F. Agullo-López, T. Torres, Chem. Rev. 104 (2004) 3723–3750
8. C.L. Jones, T. Howard, N.M. Pleasant, J. Und. Chem. Res. **8**(1), 32–36 (2009)
9. W.Y. Tong, A.B. Djurisic, A.M.C. Ng, W.K. Chan, Thin Solid Films **515**, 5270–5274 (2007)
10. M.M. El-Nahass, A.M. Farag, K.F. Abd El-Rahman, A.A.A. Darwish, Opt. Laser Technol. **37**, 513–523 (2005)
11. M. Hanack, A. Datz, R. Fay, K. Fischer, U. Keppler, J. Koch, J. Metz, M. Mezger, O. Schneider, H.J. Schulze, *Handbook on Conducting Polymers* (T. Skotheim, Ed., Marcel Dekker, New York, 1985)
12. K. Soo-Jong, M. Matsumoto, K. Shigehara, J. Porphyrins, Phthalocyanines **4**, 136–144 (2000)
13. J. Tauc, *"Optical Properties of Non-Crystalline Solids", in Optical Properties of Solids, F. Abele's (Ed.)* (North-Holland Publishing Co., Amsterdam, 1972), p. 277
14. J. Metz, M. Hanack, J. Am. Chem. Soc. **105**, 828–830 (1983)
15. L. Sutarlie, K. Yang, Sens, Actuators, B **134**, 1000–1004 (2008)
16. N.A. Rakow, A. Sen, M.C. Janzen, J.B. Ponder, K.S. Suslick, Angew. Chem. Int. Ed. **44**, 4528–4532 (2005)
17. M.-M. Shi, H.-Z. Chen, M. Wang, J. Appl. Polym. Sci. **64**(9), 1769–1774 (1997)
18. M.M. El-Nahass, M.M. Sallam, H.A. Ali, Int. J. Mod. Phys. B **19**, 4057–4071 (2005)
19. M.M. El-Nahass, A.M. Farag, K.F. Abd El-Rahman, A.A.A. Darwish, Optics & Laser Technol. **37**, 513–523 (2005)
20. J. Bardeen, F.J. Slatt, L.J. Hall, Photoconductivity Conference, p. 146 Wiley, New York, 1956
21. R. Rella, J. Spaavecchia, G. Ciccarella, P. Siciliano, G. Vasapollo, L. Valli, Sens. Actuators, B **89**, 86–91 (2003)
22. X. Li, H. Zhu, J. Wei, K. Wang, E. Xu, Z. Li, D. Wu, Appl. Phys. A **97**, 341–344 (2009)
23. L. Leontie, M. Caraman, M. Delibas, G.I. Rusu, Mater. Res. Bull. **36**, 1629–1637 (2001)
24. L. Leontie, M. Roman, F. Brinza, C. Podaru, G.I. Rusu, Synthetic Metals **138**, 157–163 (2003)
25. S. Ambily, C.S. Menon, Solid State Commun. **94**, 485–487 (1995)
26. A.K. Abass, A. Krier, R.A. Collins, Phys. Status Solidi. A **142**, 435–442 (1994)
27. G.D. Cody. Hydrogenated Amorphous Silicon, Part B, Optical Properties, Semiconductors and Semimetals, vol. 21, Ed. J. I Pankove, Academic Press, Orlando, 1984
28. M.S. Kiani, G.R. Mitchell, Synth. Met. **46**, 293–306 (1992)
29. A. Kumnar Mahapatro, S. Ghosh, J. Appl. Phys. 101 (2007) 034318-1-034318-5
30. R. Seoudi, G.S. El-Bahy, Z.A. El Sayed, J. Mol. Struct. **753**, 119–126 (2005)
31. K.R. Rajesh, C.S. Menon, Can. J. Phys. **83**, 1151–1159 (2005)